Magnetic and Mössbauer effect studies of ZnO thin film implanted with iron ions to high fluence

2017 J. Phys.: Conf. Ser. 789 012072

(http://iopscience.iop.org/1742-6596/789/1/012072)

Magnetic and Mössbauer effect studies of ZnO thin film implanted with iron ions to high fluence

A L Zinnatullin[1], A I Gumarov[1], I F Gilmutdinov[1], V F Valeev[2], R I Khaibullin[2] and F G Vagizov[1]

[1] Kazan (Volga Region) Federal University, Kremlevskaya 18, 420008 Kazan, Russia
[2] Zavoysky Physical-Technical Institute, Sibirsky Trakt 10/7, 420029 Kazan, Russia

E-mail: almaz.zinnatullin@gmail.com

Abstract. We present the results of magnetic and Mössbauer effect studies of zinc oxide thin film obtained by RF magnetron sputtering and implanted with 40 keV iron ions to a fluence of $1.5 \cdot 10^{17}$ ion/cm^2. As-implanted and post-annealed sample shows ferromagnetic properties at room temperature and consists of paramagnetic and ferromagnetic phases according to Mössbauer spectroscopy.

1. Introduction

There has been considerable interest to materials that show semiconducting and magnetic properties simultaneously. Materials with this combination of properties can be used to create spintronic devices such as spin field effect transistor (spin-FET). Such materials should have the relative long spin coherence length of electrons, otherwise, information carried by each spin will be distorted. Therefore, these materials should have homogeneous crystal structure. On the other hand, it is necessary to have the ferromagnetic properties of these materials at room temperature for creating the functional devices [1]. T. Dietl et al. [2] predicted that few semiconductors doped with "magnetic" ions can show room temperature ferromagnetic behavior. The prediction stimulated intensive research devoted to the theoretical and experimental investigations of materials called as diluted magnetic semiconductors (DMS). Iron doped zinc oxide (ZnO) is one of such materials.

We investigated the ZnO thin film implanted with iron ions. Magnetic properties were measured by vibrating sample magnetometer (VSM). Phase composition and valence state of implanted iron ions were studied by room-temperature conversion electron Mössbauer spectroscopy (CEMS).

2. Sample preparation

ZnO thin film with the thickness of 130 nm was deposited by RF magnetron sputtering on monocrystalline silicon (100) substrate at room temperature. The film was grown under the pressure of $5 \cdot 10^{-3}$Torr in the *BESTEC* vacuum system. Magnetron power was about 100 W. Then, the ZnO film was implanted with 40 keV iron ions (enriched with Fe^{57} isotopes up to 40 %) to a fluence of $1.5 \cdot 10^{17}$ ions/cm^2 in the *ILU-3* ion accelerator (Zavoysky Physical-Technical Institute). The ion implantation was carried out at room temperature and ion beam current density was 8 μA/cm^2. The subsequent annealing of the sample was performed in high vacuum (~10^{-8} Torr) at 500 °C for half an hour.

3. Results and discussion

CEMS measurements of ^{57}Fe nuclei were performed using constant acceleration spectrometer (WissEl) employing ^{57}Co embedded in Rh matrix source. All measurements were carried out at room temperature. CEMS spectra of the sample before and after annealing are presented on figure 1. They consist of one sextet with wide distribution of hyperfine magnetic field on iron nuclei and two doublets. The best fits of experimental data were achieved under assumption of the non-symmetric Gauss distribution of hyperfine magnetic field on ^{57}Fe nuclei. The obtained non-symmetric distributions are wider on the side of lower fields. The hyperfine parameters of the ascertained components are presented on table 1.

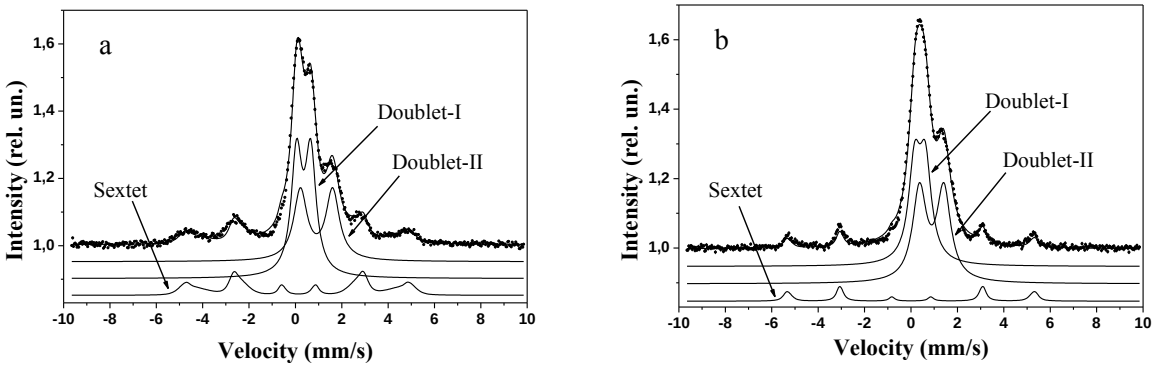

Figure 1. Room-temperature CEMS spectra of ZnO thin film implanted with iron ions with energy 40 keV to the fluence of $1.5 \cdot 10^{17}$ ions/cm^2 (a) - before annealing and (b) - after annealing at 500 °C for 30 minutes.

The sextets in Mössbauer spectra correspond to the magnetically ordered phases of the sample. The hyperfine parameters of the sextet for as-implanted sample (δ = 0.11 mm/s, ΔE_Q =- 0.06mm/s, B_{hf} = 290 kOe) are a slightly different from the well known parameters for iron-based bulk phases. However, they are close enough to the parameters which characterize the ensemble of small metallic iron nanoparticles with a wide particle size distribution. In this case, an appreciable amount of iron atoms can be located on the shell of nanoparticles and between these magnetically ordered nanoparticles. These circumstances lead to a decrease of the average hyperfine magnetic field, $<B_{hf}>$, and to a positive value of the average isomer shift δ of the ensemble of atoms relative to the bulk α-Fe.

Table 1. Hyperfine parameters of identified phases.

Sample	Component of the spectrum	Valence state of iron	$<B_{hf}>$, kOe	δ, mm/s	ΔE_Q, mm/s	Relative content, %
$1.5 \cdot 10^{17}$ions/cm^2 as-implanted	Sextet	Fe^{+3} or Fe^0	290	0.11	-0.06	32.8
	Doublet-I	Fe^{+3}	-	0.36	0.61	45.2
	Doublet-II	Fe^{+2}	-	0.91	1.39	22
$1.5 \cdot 10^{17}$ions/cm^2 post-annealed	Sextet	Fe^0	331	0	-0.02	15.8
	Doublet-I	Fe^{+3}	-	0.39	0.46	49.6
	Doublet-II	Fe^{+2}	-	0.89	1.05	34.6

$<B_{hf}>$ - average hyperfine magnetic fields on iron nucleus, δ –isomer shift relative to α-Fe, ΔE_Q–quadrupole splitting

The hyperfine parameters of the sextet for the annealed sample are in good agreement with the parameters of the metallic iron. This is probably due to the fact that an increase of thermal energy leads to the intensification of the diffusion processes, which causes the aggregation of dispersed metallic iron as well as the growth of magnetic clusters in size. The distribution of hyperfine fields becomes significantly narrower after subsequent annealing (figure 1). It should be noted that the relation of intensities for 1 and 2 lines (as well as for 5 and 6) of sextet is equal to 3:4. In our

experiment the propagation direction of the gamma photons is perpendicular to the sample plane, so this ratio is possible only when the magnetic moments of the iron atoms are in plane of the sample.

The presence of doublets in the spectrum is usually associated with the formation of paramagnetic iron phases. In earlier papers [4, 5] was shown that the implantation of Fe^+ ions into ZnO single crystal leads to the formation of metallic iron and zinc ferrite ($ZnFe_2O_4$) nanoparticles. The hyperfine parameters of the weakly split doublet (δ = 0.36 mm/s, ΔE_Q = 0.61 mm/s) indicated in the spectrum as "Doublet-I", are very close to the parameters of the $ZnFe_2O_4$ particles [4]. Subsequent vacuum annealing increases the content of this phase for 4.4%.

The vacuum annealing caused more pronounced effect on the relative content of the magnetically ordered phase and paramagnetic phase of the iron atoms in the divalent state. The relative content of magnetically ordered phase decreases about 17%, whereas the content of the paramagnetic phase (Doublet-II) increases up to 12.6%.. Last one may be associated with the formation of the Fe_xO nanoparticles during the implantation process [6]. The revealed growth of its content after annealing can be explained by the oxidation of the metallic iron nanoparticles. The origin of these paramagnetic doublets is not clear and requires further detailed studies of the symmetry and the local environment of iron atoms.

Magnetic studies were performed with a vibrating sample magnetometer (PPMS-9, Quantum Design). Magnetization curve versus magnetic field are obtained. Measurements were carried out at 10 K and room temperature (figure 2). Parameters of hysteresis loops are shown on the table 2.

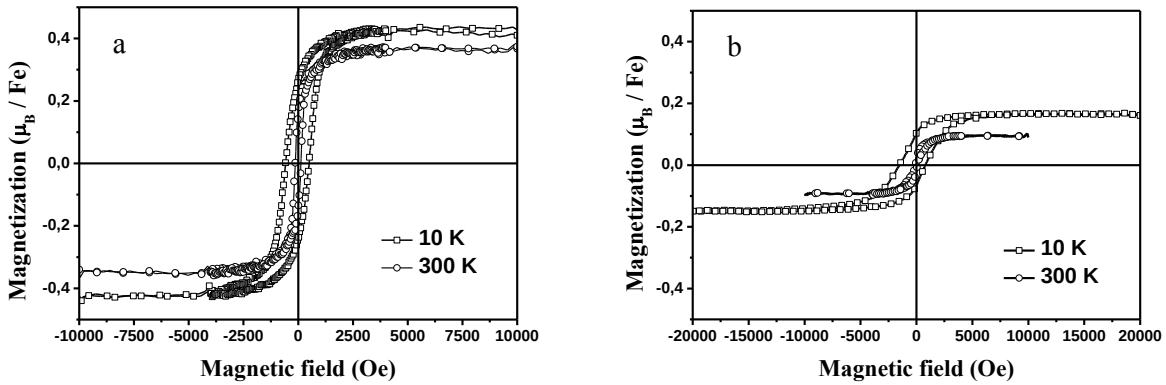

Figure 2. Magnetic hysteresis loops of ZnO thin film implanted with the 40 keV iron ions to the fluence of $1.5 \cdot 10^{17}$ ions/cm^2 (a) - before annealing and (b) - after annealing at 500 °C for 30 minutes.

It is seen that the sample under study exhibit the ferromagnetic properties before and after annealing even at room temperature. The saturation magnetization and the coercive field values of hysteresis loops increase while the temperature decrease. The annealed sample has a smaller value of the saturation magnetization.

Table 2. Magnetic hysteresis loops parameters.

Sample	Measuring temperature, K	Coercive field, Oe	Saturation magnetization, μ_B/Fe	Remnant magnetization, μ_B/Fe
$1.5 \cdot 10^{17}$ions/cm^2	10	504	0.43	0.26
as-implanted	300	133	0.37	0.17
$1.5 \cdot 10^{17}$ions/cm^2	10	810 (-1487)	0.17	0.10
post-annealed	300	109	0.10	0.02

Hysteresis loop of the annealed sample at 10 K is shifted to smaller magnetic fields. This shift may arise due to exchange bias. Exchange bias occurs in the case of the tight magnetic contact between the ferromagnetic and antiferromagnetic phases. The exchange interaction at the boundary of two types of magnets may lead to appearance of the preferred directions of the magnetization vector at low

temperatures. Typically exchange anisotropy arises in "core-shell" nanoparticles, where the pair of two types of magnets is formed due to the oxidation of the surface of the nanoparticles [7]. In our case, a surface of the ferromagnetic iron nanoparticles can be oxidized to antiferromagnetic FeO phase.(For the bulk FeO the Neel temperature is about 198 K[6]).

4. Conclusion

Zinc oxide thin film prepared by RF magnetron sputtering technique and post-implanted with 40 keV iron ions to fluence of $1.5 \cdot 10^{17}$ ions/cm^2 has been studied. The implanted sample exhibits the ferromagnetic properties at room temperature. The iron nanoparticles are primary source of room temperature ferromagnetism. Composition of iron-containing phases in Fe-implanted ZnO film consists of magnetically ordered and paramagnetic phases. Vacuum annealing reduces the content of the magnetically ordered phase. Magnetic properties of iron nanoparticles embedded inside ZnO can be tuned by vacuum annealing.

Acknowledgments

The authors acknowledge support by the Program of Competitive Growth of Kazan Federal University. The Mössbauer and magnetic measurements were carried out at the PCR Federal Center of Shared Facilities of KFU.

References

[1] Wolf S A, Awschalom D D, Buhrman R A, Daughton J M, von Molnár S, Roukes M L, Chtchelkanova A Y and Treger D M 2001 *Science* **294** 1488
[2] Dietl T, Ohno H, Matsukura F, Cibert J and Ferrand D 2000 *Science* **287** 1019
[3] Lyadov N M, Bazarov V V, Vagizov F G, Vakhitov I R, Dulov E N, Kashapov R N, Noskov A I, Khaibullin R I, Shustov V A and Faizrakhmanov I A 2016 *Applied Surface Science* **378** 114
[4] Zhou S, Potzger K, Reuther H, Talut G, Eichhorn F, von Borany J, Skorupa W, Helm M and Fassbender J 2007 *Journal of Physics D: Applied Physics* **40** 964
[5] Potzger K, Zhou S, Reuther H, Muecklich A, Eichhorn F, Schell N, Skorupa W, Helm M, Fassbender J, Herrmannsdoerfer T and Papageorgiou T P 2006 *Applied Physics Letters* **88** 052508
[6] Kozioł-Rachwał A, Ślęzak T, Nozaki T, Yuasa S and Korecki J 2016 *Applied Physics Letters* **108** 041606
[7] Noguésa J and Schuller I 1999 *Journal of Magnetism and Magnetic Materials* **192** 203